Analysis of food appearance properties by computer vision applying ellipsoids to colour data

Rodríguez-Pulido, Francisco J.; Gordillo, Belén; González-Miret, M. Lourdes.; Heredia, Francisco J.

Food Colour & Quality Lab., Dept. Nutrition & Food Science. Facultad de Farmacia. Universidad de Sevilla. 41012-Sevilla, Spain.

Corresponding author:
Heredia, Francisco J.;
Food Colour & Quality Lab., Dept. Nutrition & Food Science. Facultad de Farmacia. Universidad de Sevilla. 41012-Sevilla, Spain
Tel.: +34 954556495 Fax: +34 954556110
e-mail: heredia@us.es

ABSTRACT

The use of computer vision for estimating composition in food products has become wide spread in recent years, especially for products where by measuring colour or other spectral features, we are able to estimate the composition, variety, or ripeness. On the other hand, the appearance is one of the most worrying issues for producers due to its influence on quality and consumer preferences. Computer vision is the best option to satisfy the need of measuring colour and heterogeneity in these products. Previous studies have expressed the heterogeneity with the standard deviation or other magnitudes that do not explain accurately the distribution of colour in CIELAB colour space. Graphing the scatterplot of the a*b* values belonging to the pixels of the image helps to explain the shape of the point cloud, but currently there is not an objective procedure to quantify these point clouds. This work has established a method for improving the illustration of colour measurements by image analysis. The proposed algorithm classified the point clouds by clustering methods and established the methodology for fitting the resulting clusters into ellipsoids. Their geometric features described the shape of the clouds in a quantitatively manner and they could be useful in multivariate statistical techniques for classifying and predicting chemical properties.

KEYWORDS

Food colour; colour ellipsoids; CIELAB; image analysis; clustering.

1. INTRODUCTION

Computer vision has radically changed the outlook of evaluating the composition of food products in recent years. Its advances have improved within the framework of accuracy, and joined to chemometrics, 'Chemical Imaging' is widely used nowadays (ElMasry & Sun, 2010). The higher requirements on quality control has entailed that it is not enough analysing only the chemical composition but also the spatial distribution within a sample (Du & Sun, 2004). The relationship between chemical composition and spectral properties have been well studied in infrared and visible spectra by several techniques, such as near infrared spectroscopy, near infrared reflectance spectroscopy, and visible and infrared hyperspectral imaging (Hernández-Hierro et al., 2012; Rodríguez-Pulido et al., 2012; Barbin, ElMasry, Sun, & Allen, 2013; Mathiassen, Misimi, Bondø, Veliyulin, & Østvik, 2011; Mathiassen et al., 2011; Romano, Argyropoulos, Nagle, Khan, & Müller, 2012). Besides of composition, these measurements are important since food appearance is one of the most important characteristics due to its relationship with quality and consumer preferences (Fernández-Vázquez, Stinco, Meléndez-Martínez, Heredia, & Vicario, 2011; Calvo, Salvador, & Fiszman, 2001). Since food industry includes products having very different sizes and shapes, computer vision arises as a suitable option to satisfy the need of measuring colour regardless the nature of samples. Moreover, computer vision allows measuring not only colour but also other features related to appearance, that do not vary the colour, but they affect to how the human eye perceive it, such as texture or heterogeneity (Valous, Mendoza, Sun, & Allen, 2009).

Back in 1942, David L. MacAdam used ellipsoids for marking regions in colour spaces having common properties (MacAdam, 1942). In that study, the standard deviations were represented in terms of distance in the CIE 1931 colour space chromaticity diagram and these regions were fitted into ellipses. They showed that sources radiating spectral distributions belonging to these regions of the diagram appeared to have the same colour, for the average human observer. Later, some authors used a "closest packing"lattice of points to improve the understanding of the space involved by ellipsoids (Salmerón et al., 2012; Wyszecki, 1954; MacAdam, 1974; Luke, 1999; Judd & Wyszecki, 1975). In these cases, the lattice constant might represent the smallest number of just-noticeable chromaticity steps between the two chromaticities represented by the two points

In computer vision, device-dependent colour spaces are commonly employed in image analysis because this kind of information is given by cameras directly (Jack, 2008). Nevertheless, colour must be measured by device-independent colour spaces (its appearance does not depend on the device) to ensure the objectivity of the measure. Among these spaces, CIELAB is one of the colour spaces recommended by the International Commission on Illumination (CIE) and it is considered perceptually uniform, meaning that just-detectable visual difference constitutes a constant distance in any location or direction within the space (CIE, 1976). Therefore CIELAB is widely used as a standard space for comparing colours because of its reliability.

Within CIELAB, a psychometric index of lightness (L*) and two colour coordinates (a* and b*) are defined. L* is the quantitative attribute of relative luminosity, which is the property according to which each colour can be considered as equivalent to a member of the grey scale, ranging between black ($L^*=0$) and white ($L^*=100$). Coordinate a^* takes positive values for reddish colours and negative values for greenish ones, and b^* takes positive values for yellowish colours and negative values for bluish ones. From the Cartesian coordinates (a^* and b^*), two angular parameters can be defined: chroma and hue or hue angle. Hue angle (h_{ab}) is the qualitative attribute that allows any colour to be graded as reddish, greenish, etc., and chroma (C^*_{ab}) is considered the quantitative attribute of colourfulness, allowing assessing the degree of difference of any given hue relative to a grey colour with the same lightness (Hutchings, 1999).

Obtaining the CIELAB coordinates by image analysis requires a camera which records visible light in gradations of three basic colours: red, green and blue (RGB). This device-dependent colour space may be transformed into CIELAB coordinates by means of a calibration which in turn requires controlled lighting (CIE, 2007; León, Mery, Pedreschi, & León, 2006). After taking images and transforming between colour spaces, a segmentation criterion is applied for calculating colour only from pixels with analytical information, also known as region of interest (ROI). There are different techniques of segmentation, being thresholding and edge-detection the main ones (Cheng, Jiang, Sun, & Wang, 2001; Zheng & Sun, 2008).

Since colour can be extracted from each pixel of the ROI, some variables emerge in order to express the degree of heterogeneity. Most of the studies show the result of measurements as the average colour and its standard deviation from all the pixels selected of the ROI (Yam & Papadakis, 2004; Valous et al., 2009; Mendoza, Dejmek, & Aguilera, 2006; Girolami, Napolitano, Faraone, & Braghieri, 2013; Dufossé, Galaup, Carlet, Flamin, & Valla, 2005), being this standard deviation mainly a consequence of the heterogeneity instead of the measuring error. Besides the standard deviation, there are more scalar magnitudes in order to quantify the heterogeneity of samples, such as the mean colour difference from the mean (MCDM) (Berns, 2000) and entropy, which is dimensionless (Arzate-Vázquez et al., 2011). Further than a simple point plus a scalar explaining its heterogeneity, some authors resort to graph the scatterplot of the a*b* values as a point cloud, corresponding the points to the colour of each pixel (Urban, Berns, & Grigaf, 2007; Palus, 2006). This option is quite useful, because these graphs are fairly explanatory and give an idea about the colours present in the sample as well as the relative presence of each one. However, a problem arises when the colour of a sample is spread out in two or more different point clouds. In these cases, the average colour may represent a point that cannot even be present in the sample. Currently, there are not objective procedures for discerning how many groups of colours are present in a sample. Some authors have used clustering methods on image analysis, not for classifying colours but for segmentation or detection purposes (Li, Wang, Wang, & Li, 2012; Yin, Chai, Yang, & Mittal, 2011).

This work has established an easy to carry out methodology for improving the evaluation of heterogeneous colours in food products and the illustration of these measurements in CIELAB colour space. The proposed algorithm could be useful for obtaining analytical information in studies where by chemometrics, the relationship among colour, appearance, and composition wants to be studied.

2. MATERIAL AND METHODS

2.1 Imaging system

For acquiring images, the DigiEye® system based upon a calibrated digital camera was used (Luo, Cui, & Li.C, 2001). It includes an illumination box specially designed by VeriVide Ltd. (Leicester, UK) to illuminate the samples consistently and a digital camera connected to a computer. The digital camera used for image acquisition was a 10.2-megapixel Nikon® D80 with Nikkor® 35 mm f/2D objective. It was calibrated with the DigiTizer (VeriVide Ltd., Leicester, UK) colour chart with the aim of characterize the camera response by relating its RGB signals to CIE specifications. The cabinet is equipped with two fluorescent tubes that emulate the CIE standard illuminant D65 and offer stable lighting conditions (CIE, 2007). They were switched on at least ten minutes before being used, according to manufacturer indications, to stabilize them.

The application of the methodology and the algorithm for computing the ellipsoids from point clouds were developed on MATLAB (The Mathworks, 2009). Within MATLAB, the Fuzzy Logic, Image Processing, Partial Differential Equation and Statistics Toolboxes were also used.

The aim of this work was the establishment of a new methodology for the interpretation of the colour heterogeneity, so the development of the method and its application to different food samples have been included in the Results section.

2.2 Samples

The algorithm was applied to food products having different size and appearance for showing the results in a clear manner. Cabbages (*Brassica oleracea* var. Viridis), oranges (*Citrus sinensis* L. Osbeck var. Navelate), apples

(*Malus domestica* var. Kanzi), and tomatoes (*Solanum lycopersicum* L. var. Kumato) purchased from local retailers were studied. Seeds from red grapes (*Vitis vinifera* var. Syrah) were included as representative of small-size samples. These fruits and vegetables were chosen based on the representativeness of foodstuff having different colour and heterogeneity. Homogeneous food products such as wines or juices were not considered since the evaluation of heterogeneity in this type of samples has not sense.

For proving the potential of the method, the sugar content of grapes, which is an indicator of maturity in oenology, was estimated by means of the proposed method. For this purpose, 254 white grapes (Vitis vinifera var. Zalema) were taken at nine dates during the interval of time where the change of colour occurs. The vineyards sampled are included under the “Condado de Huelva” Designation of Origin, in Southwestern Spain, harvested in 2012. As reference method, an Abbe refractometer was used to evaluate the sugar concentration according to the method of The International Organisation of Vine and Wine (OIV, 2013).

3. RESULTS

3.1 Methodological procedure

3.1.1 Image acquisition

As is usual in computer vision, the images were acquired under diffuse illumination for avoiding undesired glints and shadows. The background were chosen for make easier the segmentation process, to the extent possible. A thick sheet was used for this purpose since it is considered a good Lambertian surface (diffuse reflectance surface which does not vary depending on the viewing angle) (Jaglarlz, Duraj, Szopa, Cisowski, & Czternastek, 2006).

3.1.2 Segmentation

The segmentation criteria depend on nature of samples. In this case, and based on the chromatic differences among samples and background, the pixels having the ratio C^*_{ab}/L^* higher than 2.6 CIELAB units was chosen as segmentation criterion. Then, the inner holes in segmentation mask were filled, and the resulting regions were eroded in order to avoid possible aberration of colours at the edge of the objects.

3.1.3 Clustering

The methodology proposed by Yager and Filev (1994) was followed for the clustering process. This subtractive clustering method assumes that each point is a potential cluster centre and calculates a measure of likelihood that each data point would define the cluster centre, based on the density of surrounding data points. It can be summarized in three steps. In the first step it discretizes the object space and in doing so, it generates the potential cluster centres. For locating the next data cluster and its centre position, the second step removes all data points in the vicinity of the first cluster centre. Finally, it iterates on this process until all data are under the influence of a cluster centre. Due to all data were included in the same bidimensional space, the range of influence was set in agreement with the acceptable tolerance by the human eye (Martínez, Melgosa, Pérez, Hita, & Negueruela, 2001).

3.1.4 Fitting to ellipsoids

Each cluster was composed by a $(m \times 3)$-matrix containing the CIELAB colorimetric variables of the points:

$$\mathrm{cluster_n} = \begin{pmatrix} L_1^* & a_1^* & b_1^* \\ L_2^* & a_2^* & b_2^* \\ \vdots & \vdots & \vdots \\ L_i^* & a_i^* & b_i^* \\ \vdots & \vdots & \vdots \\ L_m^* & a_m^* & b_m^* \end{pmatrix}_{mx3} \qquad \text{Eq. 1}$$

From each cluster, the orientation of the ellipsoid with respect to the (a*b*)-plane was calculated by robust linear regression of the points. This regression improved the result calculated by simple linear regression, removing the effects of outliers. The orientation, in degrees, was calculated by the expression:

$$\theta = \operatorname{atan} b \qquad \text{Eq. 2}$$

being *b* the slope obtained by the regression. Each row of the matrix was multiplied by the rotation matrix *R*. The new points *(L*,a*',b*')* had not colorimetric sense, but they were useful for calculating the axes of the ellipsoid:

$$\boldsymbol{R} = \begin{pmatrix} 1 & 0 & 0 \\ 0 & \cos\theta & -\sin\theta \\ 0 & \sin\theta & \cos\theta \end{pmatrix} \qquad \text{Eq. 3}$$

$$\begin{pmatrix} L_i^* & a_i^{*'} & b_i^{*'} \end{pmatrix} = \begin{pmatrix} L_i^* & a_i^* & b_i^* \end{pmatrix} \times \begin{pmatrix} 1 & 0 & 0 \\ 0 & \cos\theta & -\sin\theta \\ 0 & \sin\theta & \cos\theta \end{pmatrix} \qquad \text{Eq. 4}$$

Thus, the centre of the ellipsoid was located at:

$$\mathrm{Centre} = \left(\bar{L}^*, \bar{a}^*, \bar{b}^*\right) \qquad \text{Eq. 5}$$

and the dimensions of the ellipsoid along the direction defined by θ were defined by:

$$\mathrm{Length} = 2 \times \left[\frac{1}{m-1} \sum_{i=1}^{m} \left(a_i^{*'} - \bar{a}^{*'}\right)^2\right]^{\frac{1}{2}} \qquad \text{Eq. 6}$$

$$\text{Width} = 2 \times \left[\frac{1}{m-1} \sum_{i=1}^{m} \left(b_i^{*'} - \bar{b}^{*'} \right)^2 \right]^{\frac{1}{2}} \quad \text{Eq. 7}$$

$$\text{Height} = 2 \times \left[\frac{1}{m-1} \sum_{i=1}^{m} \left(L_i^{*} - \bar{L}^{*} \right)^2 \right]^{\frac{1}{2}} \quad \text{Eq. 8}$$

The axes of the ellipsoid were set to two standard deviations, where about 95% of the values lie within this scope in a normal distribution.

3.2 Application of the methodology to food products

The method was applied to the following products:

For an image of a cabbage, the point cloud on the (a*b*)-plane of the points is shown in Figure 1. The colour of cabbage varied from greenish (with positive values for b* and negative ones for a*) to achromatic ones (values close to zero for a* and b*). In this case, there was a colour gradation between both areas. Nevertheless, colour might change drastically among different areas in images. In this respect, the role of the resolution of images has to be highlighted. Images having high resolution will have fewer points between point clouds than images having low one. The figure 2 shows the point cloud of an orange slice. Almost all the points are concentrated in the region of the diagram that represents typically orange colours. The white mesocarp, more achromatic, appears closer to the origin of coordinates in a small cloud. In this case, the possibility that a pixel belongs to the boundary between the endocarp and mesocarp is higher in the low resolution image. Additionally, the extension of the points belonging to orange area reduces its size in low resolution images because the representativeness of colour decreases as well (Fig. 2b).

Another example including the clustering process is shown in Figure 3. Images of grape seeds at different stages of ripeness and their point clouds after applying the clustering process are shown in Figure 3. The Figures 3a, 3b, and 3d were composed of one cluster each one. Conversely, the Figure 3c showed more heterogeneity than the others. This way, if it had been considered as a unique point cloud, it would have had a higher standard deviation, but its belonging to two clusters would not have been explained. Because this sample was composed of two independent colours, it must be considered the individual heterogeneity of each one.

On the other hand, in both orange and cabbage cases, the scatter of point has an oblique distribution. This fact involves high standard deviation in a* and b* coordinates. Nonetheless, the points representing the colour in cabbage are apparently aligned. This means that points having the same distribution will have different standard deviations depending on the orientation of the cloud. Therefore standard deviations of colorimetric coordinates are not suitable values to express the heterogeneity of colour because they do not define the actual shape of these point cloud.

The Figure 4 shows how the rotation operation aligned the point cloud with the axes. As previously described, the new position of the cloud had not colorimetric sense, but the standard deviations obtained were more consistent with the true shape of the cloud and they still had CIELAB units since only the orientation of coordinate system was modified.

The Figure 5 shows images of an apple and a tomato concluding the methodology. The algorithm categorized by clusters the point clouds and included the fitted ellipses. The image of the apple was composed by two principal clusters well defined belonging to red and yellow areas. A small region between them showed how colours gradually went from red to yellow.

Moreover, the bigger size of this intermediate ellipse indicated the greater heterogeneity of this cluster. The algorithm also classified the tomato into three clusters. Nevertheless, there was more homogeneity regarding the size and orientation of its ellipses. The information of each ellipse is described in detail in Table 1. It is important to highlight that orientation angle has not relationship with the qualitative attribute of colour. It is used for giving an idea of the shape of the point cloud. For each cluster, the area of image belonging to this cluster, the centre of the ellipse, its dimensions, eccentricity and orientation were defined.

At this point, only variables a* and b* were taken into account. Thus the proposed ellipses were not still able to explain how large was the point cloud along the third colorimetric variable, lightness (L*). With the aim of evaluating the distinguishable colours that contains each cluster, the ellipses became into ellipsoids by considering the variable L*, building this dimension with the same criterion which the others axes were built. The CIELAB colour space is continuous, meaning that there is an infinite number of colours points within every portion of space considered. Nonetheless, there must be a minimal difference of colour (ΔE) for being noticeable by the human eye. According to Martínez *et al.* (2001), a value around 3.0 CIELAB units should be considered a preliminary estimate of the acceptable tolerance by a non-trained person in wines. This way, the volume of ellipsoids was filled with a regular rhombohedral (cubo-octahedron) lattice of points. This lattice is a type of “closest packing”, where each point is surrounded by 12 equidistant nearest neighbours, being the distance between points called the *lattice constant*. In our case, this parameter was set at three CIELAB units. The Figure 6 shows the ellipsoids obtained for the apple (a) and the tomato (b). The projection of the lattice on the plane a*b* shows the dimension of the lattice constant, where every point represents an individual colour within each cluster. It is worthy remarkable that although the ellipsoids belonging to clusters orange and yellow look overlapped, they actually do not coincide because they are at different heights (different L* values). The lower standard deviation of points of clusters in tomato expresses itself as fewer points in the lattices built (Table 2). Anyhow, the lattice constant set at three units could be changed depending on the purpose of the study or the kind of samples in further works.

For testing the ability of the method, the ellipsoids of colour were obtained of grapes as well as their sugar concentration. The Table 3 summarises these data regarding the sampling date. The position as well as the shape of ellipsoids changes along the ripening of white grapes, and it is shown in Figure 7. Then, the sugar concentration was estimated by partial least squares regression (PLSR). Data of sugar content was used as dependent (Y) variable and data of ellipsoids of colour was used as the independent (X) variables in the PLSR. Sugar concentration, which ranged between 5.5 and 18.0 °Brix, had R^2=0.986 for calibration and R^2=0.960 for cross-validation. In turn, the root mean square error (RMSE) was 0.5 °Brix for calibration and 0.9 °Brix for cross-validation.

4. CONCLUSIONS

A novel method for estimating the number of colour groups, and therefore regions having different chemical composition, that are present in an image has been established. This method was based on a subtractive clustering method considering the threshold of perception of the human eye. On the other hand, an objective way for quantifying the resulting point clouds based on the construction of ellipsoids was developed. The orientation and semi-axes of these ellipsoids were faithfully in agreement with the actual shape of the cloud, and improved the explanation of the heterogeneity that a single point and the standard deviation provide. The method was successfully applied in images of foodstuff having different sizes, colours, and textures. Since heterogeneity may be explained quantitatively by means of new variables, these could be taken into account for being included as new variables in multivariate statistical techniques for classifying and predicting properties in food products.

ACKNOWLEDGEMENTS

This work was supported by the projects P10-AGR6331 (Consejería de Economía, Innovación, Ciencia y Empresa, Junta de Andalucía), AGL2011-30254-C02 (Ministerio de Economía y Competitividad, Gobierno de España), and the concession of the fellowship BES-2009-025429.

REFERENCES

Arzate-Vázquez, I., Chanona-Pérez, J. J., de Perea-Flores, M. J., Calderón-Domínguez, G., Moreno-Armendériz, M. A., Calvo, H. et al. (2011). Image Processing Applied to Classification of Avocado Variety Hass (Persea americana Mill.) During the Ripening Process. *Food and Bioprocess Technology, 4,* 1307-1313.

Barbin, D. F., ElMasry, G., Sun, D. W., & Allen, P. (2013). Non-destructive determination of chemical composition in intact and minced pork using near-infrared hyperspectral imaging. *Food Chemistry, 138,* 1162-1171.

Berns, R. (2000). *Billmeyer and Saltzman's principles of color technology*. Willey, New York.

Calvo, C., Salvador, A., & Fiszman, S. M. (2001). Influence of colour intensity on the perception of colour and sweetness in various fruit-flavoured yoghurts. *Eur Food Res Technol, 213,* 99-103.

Cheng, H. D., Jiang, X. H., Sun, Y., & Wang, J. (2001). Color image segmentation: advances and prospects. *Pattern Recognition, 34,* 2259-2281.

CIE (1976). *Recommendations on Uniform Color Spaces, Color-Difference Equations, Psychometric Color Terms*. Vienna: Bureau Central de la CIE.

CIE. (2007). Commission internationale de l'Eclairage. Standard Illuminants for Colorimetry. ISO 11664-2:2007.

Du, C. J. & Sun, D. W. (2004). Recent developments in the applications of image processing techniques for food quality evaluation. *Trends in Food Science & Technology, 15,* 230-249.

Dufossé, L., Galaup, P., Carlet, E., Flamin, C., & Valla, A. (2005). Spectrocolorimetry in the CIE L*a*b* color space as useful tool for monitoring the ripening process and the quality of PDO red-smear soft cheeses. *Food Research International, 38,* 919-924.

ElMasry, G. & Sun, D. W. (2010). Meat Quality Assessment Using a Hyperspectral Imaging System. In P. D.-W. Sun (Ed.), *Hyperspectral Imaging for Food Quality Analysis and Control* (pp. 175-240). San Diego: Academic Press.

Fernández-Vázquez, R., Stinco, C., Meléndez-Martínez, A. J., Heredia, F. J., & Vicario, I. M. (2011). Visual and instrumental evaluation of orange juice color: A consumers' preference study. *Journal of Sensory Studies, 26,* 436-444.

Girolami, A., Napolitano, F., Faraone, D., & Braghieri, A. (2013). Measurement of meat color using a computer vision system. *Meat Science, 93,* 111-118.

Hernández-Hierro, J. M., Valverde, J., Villacreces, S., Reilly, K., Gaffney, M., González-Miret, M. L. et al. (2012). Feasibility study on the use of visible-near-infrared spectroscopy for the screening of individual and total glucosinolate contents in broccoli. *Journal of Agricultural and Food Chemistry, 60,* 7352-7358.

Hutchings, J. (1999). *Food Color and Appearance*. (2 ed.) Springer.

Jack, K. (2008). Color Spaces. In *Digital Video and DSP* (pp. 15-29). Burlington: Newnes.

Jaglarlz, J., Duraj, R., Szopa, P., Cisowski, J., & Czternastek, H. (2006). Investigation of white standards by means of bidirectional reflection distribution function and integrating sphere methods. *Optica Applicata, 36,* 97-103.

Judd, D. B. & Wyszecki, G. (1975). *Color in business, science, and industry*. Wiley.

OIV (2013). *Compendium of international methods of wine and must analysis.* The International Organisation of Vine and Wine, Paris.León, K., Mery, D., Pedreschi, F., & León, J. (2006). Color measurement in L*a*b* units from RGB digital images. *Food Research International, 39,* 1084-1091.

Li, C., Wang, B., Wang, J., & Li, F. (2012). Extracting vein of leaf image based on K-means clustering. *Nongye Gongcheng Xuebao/Transactions of the Chinese Society of Agricultural Engineering, 28,* 157-162.

Luke, J. T. (1999). OSA Instrumental in Development of the uniform color scales. *Optics and Photonics News, 10,* 28-33.

Luo, M. R., Cui, G. H., & Li.C. (4-10-2001). British Patent entitled Apparatus and method for measuring colour (DigiEye System), Derby University Enterprises Limited.

MacAdam, D. L. (1942). Visual Sensitivities to Color Differences in Daylight. *Journal of the Optical Society of America, 32,* 247-273.

MacAdam, D. L. (1974). Uniform color scales. *Journal of the Optical Society of America, 64,* 1691-1702.

Martínez, J. A., Melgosa, M., Pérez, M. M., Hita, E., & Negueruela, A. I. (2001). Note. Visual and Instrumental Color Evaluation in Red Wines. *Food Science and Technology International, 7,* 439-444.

Mathiassen, J. R., Misimi, E., Bondø, M., Veliyulin, E., & Østvik, S. O. (2011). Trends in application of imaging technologies to inspection of fish and fish products. *Trends in Food Science & Technology, 22,* 257-275.

Mendoza, F., Dejmek, P., & Aguilera, J. M. (2006). Calibrated color measurements of agricultural foods using image analysis. *Postharvest Biology and Technology, 41,* 285-295.

Palus, H. (2006). Colorfulness of the image: Definition, computation and properties. In. Progress in Biomedical Optics and Imaging - *Proceedings of SPIE* 6158.

Rodríguez-Pulido, F. J., Ferrer-Gallego, R., González-Miret, M. L., Rivas-Gonzalo, J. C., Escribano-Bailón, M. T., & Heredia, F. J. (2012). Preliminary study to determine the phenolic maturity stage of grape seeds by computer vision. *Analytica Chimica Acta, 732,* 78-82.

Romano, G., Argyropoulos, D., Nagle, M., Khan, M. T., & Müller, J. (2012). Combination of digital images and laser light to predict moisture content and color of bell pepper simultaneously during drying. *Journal of Food Engineering, 109,* 438-448.

Salmerón, J. F., Gómez-Robledo, L., Carvajal, M. Á., Huertas, R., Moyano, M. J., Gordillo, B. et al. (2012). Measuring the colour of virgin olive oils in a new colour scale using a low-cost portable electronic device. *Journal of Food Engineering, 111,* 247-254.

The Mathworks (2009). MATLAB (Version R2009b). Natik, Massachusetts: The MathWorks Inc.

Urban, P., Berns, R. S., & Grigaf, R. R. (2007). Color correction by considering the distribution of metamers within the mismatch gamut. In *Final Program and Proceedings – IS and T/SID Color Imaging Conference,* 222-226.

Valous, N. A., Mendoza, F., Sun, D. W., & Allen, P. (2009). Colour calibration of a laboratory computer vision system for quality evaluation of pre-sliced hams. *Meat Science, 81,* 132-141.

Wyszecki, G. (1954). A Regular Rhombohedral Lattice Sampling of Munsell Renotation Space. *Journal of the Optical Society of America, 44,* 725.

Yager, R. R. & Filev, D. P. (1994). Generation of Fuzzy Rules by Mountain Clustering. *Journal of Intelligent and Fuzzy Systems, 2,* 209-219.

Yam, K. L. & Papadakis, S. E. (2004). A simple digital imaging method for measuring and analyzing color of food surfaces. *Journal of Food Engineering, 61,* 137-142.

Yin, H., Chai, Y., Yang, S. X., & Mittal, G. S. (2011). Ripe tomato detection for robotic vision harvesting systems in greenhouses. *Transactions of the ASABE, 54,* 1539-1546.

Zheng, C. & Sun, D. W. (2008). Image Segmentation Techniques. In D.-W. Sun (Ed.), *Computer Vision Technology for Food Quality Evaluation* (pp. 37-56). Amsterdam: Academic Press.

FIGURE CAPTIONS

Figure 1. Image of a cabbage and its colour on the (a*b*)-plane.

Figure 2. Point clouds of a slice of orange depending on the resolution of image.

Figure 3. Image of grape seeds at different stages of ripeness and their point clouds after applying the clustering process.

Figure 4. Point cloud showing the rotation operation within the (a*b*)-plane. White arrows show the standard deviation along two axes before and after the rotation.

Figure 5. Images of food products after applying the clustering and fitting processes.

Figure 6. Orthographic projection of ellipsoids and spatial lattice on the plane a*b*. The point clouds have been removed.

Figure 7. Evolution of ellipsoids of colour of white grapes during the ripening. L* axis has been removed to get a clearer representation.

Table 1

Table 1. Cluster centres and dimensions of the fitted ellipses for images of Fig. 5. (a*, b*, and size of ellipse in CIELAB units).

	cluster	Area on image	a*	b*	Ellipse length	Ellipse width	Eccentricity	Orientation angle
APPLE	red	53.40%	38.1	25.6	10.1	6.3	0.78	26.9º
	orange	17.90%	19.0	37.0	14.4	11.3	0.56	-20.9º
	yellow	28.70%	6.1	46.6	9.0	7.5	0.62	-17.0º
TOMATO	red	45.60%	11.7	34.3	5.1	3.9	0.65	20.4º
	pale brown	19.37%	4.9	25.4	6.7	5.0	0.67	26.3º
	green	35.03%	-2.2	15.0	4.7	3.8	0.59	41.6º

Table 2

Table 2. Centres and dimensions for ellipsoids of Fig. 6. (L*, a*, b*, length, width, and height in CIELAB units. Volume in CIELAB units^3).

	cluster	L*	a*	b*	length	width	height	volume	points in lattice
APPLE	red	37.8	38.1	25.6	10.1	6.3	11.4	379.1	59
	orange	64.2	19.0	37.0	14.4	11.3	10.2	871.3	136
	yellow	53.9	6.1	46.6	9.0	7.5	16.8	594.8	93
TOMATO	red	34.0	11.7	34.3	5.1	3.9	7.4	77.2	12
	pale brown	20.1	4.9	25.4	6.7	5.0	8.0	74.9	11
	green	26.9	-2.2	15.0	4.7	3.8	6.8	119.1	18

Table 3

Table 3. Centres and dimensions for ellipsoids of Fig. 7. (L^*, a^*, b^*, length, width, and height: CIELAB units; orientation angle: degrees; volume: CIELAB units^3; the remaining magnitudes are dimensionless).

Sampling	date	°Brix	L*	a*	b*	length	width	height	eccentricity	orientation angle	volume	points in lattice
1	2-Jul	5.5	55.6	-10.6	48.1	7.8	4.1	6.5	0.85	-11.7	108.2	17
2	9-Jul	6.1	57.6	-10.6	48.4	7.1	4.6	6.6	0.76	-20.9	114.5	18
3	22-Jul	11.7	61.5	-5.4	48.7	8.7	4.5	5.6	0.86	11.2	113.6	18
4	25-Jul	12.7	62.1	-5.1	46.0	9.4	5.8	7.4	0.79	-20.0	212.2	33
5	29-Jul	13.6	62.1	-2.8	46.5	9.7	5.7	6.1	0.81	9.9	175.6	28
6	31-Jul	14.6	63.2	-2.0	46.2	9.6	5.9	5.8	0.79	0.2	173.6	27
7	5-Aug	16.1	61.3	-0.9	46.1	9.1	6.7	6.4	0.67	-3.9	202.7	32
8	8- Aug	16.2	62.7	-0.1	45.7	8.4	5.6	6.6	0.75	-3.0	160.7	25
9	12- Aug	18.0	61.7	0.5	46.9	7.5	5.3	6.8	0.71	-2.7	140.9	22

Figure 1
Click here to download high resolution image

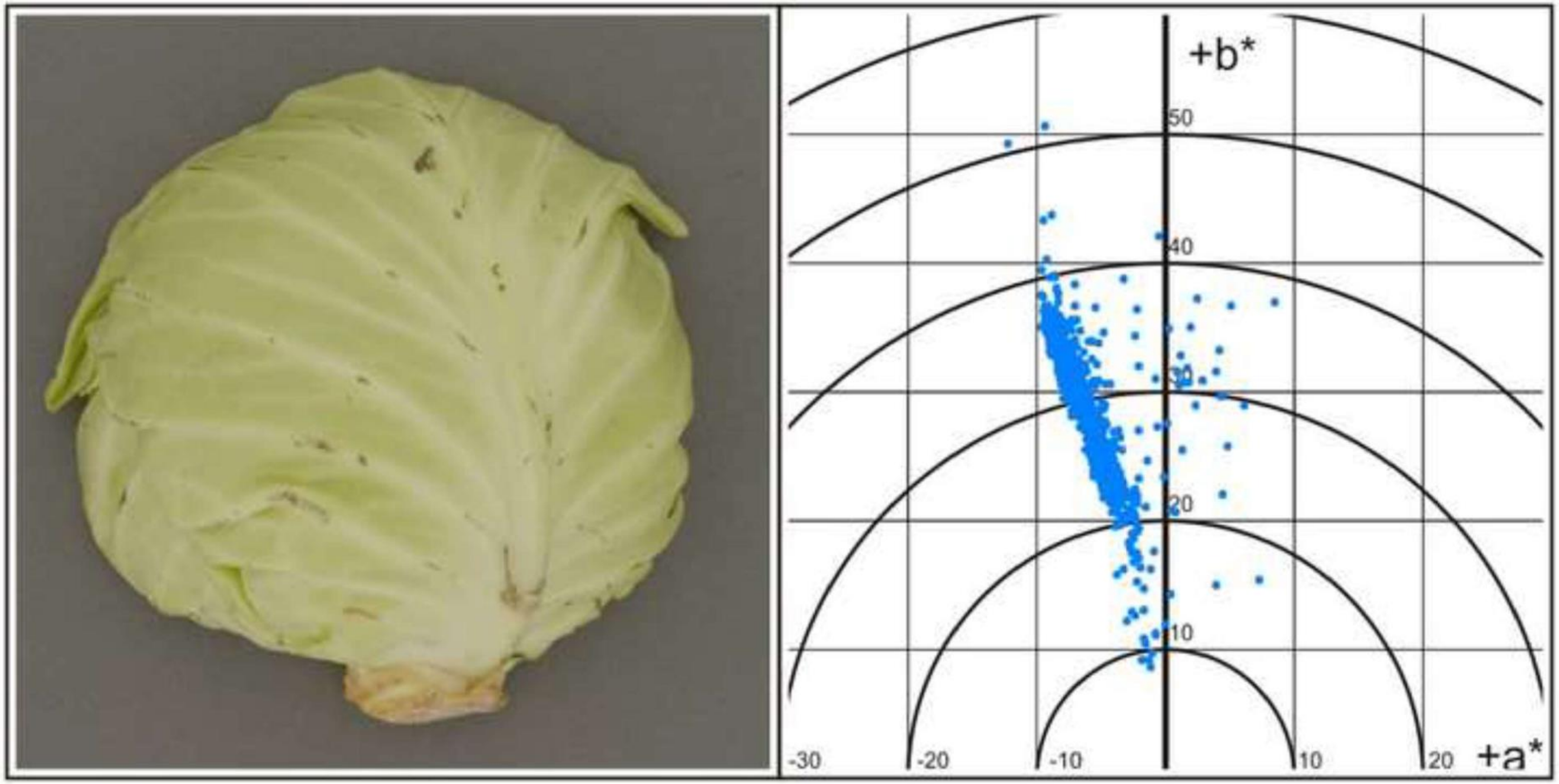

Figure 2
Click here to download high resolution image

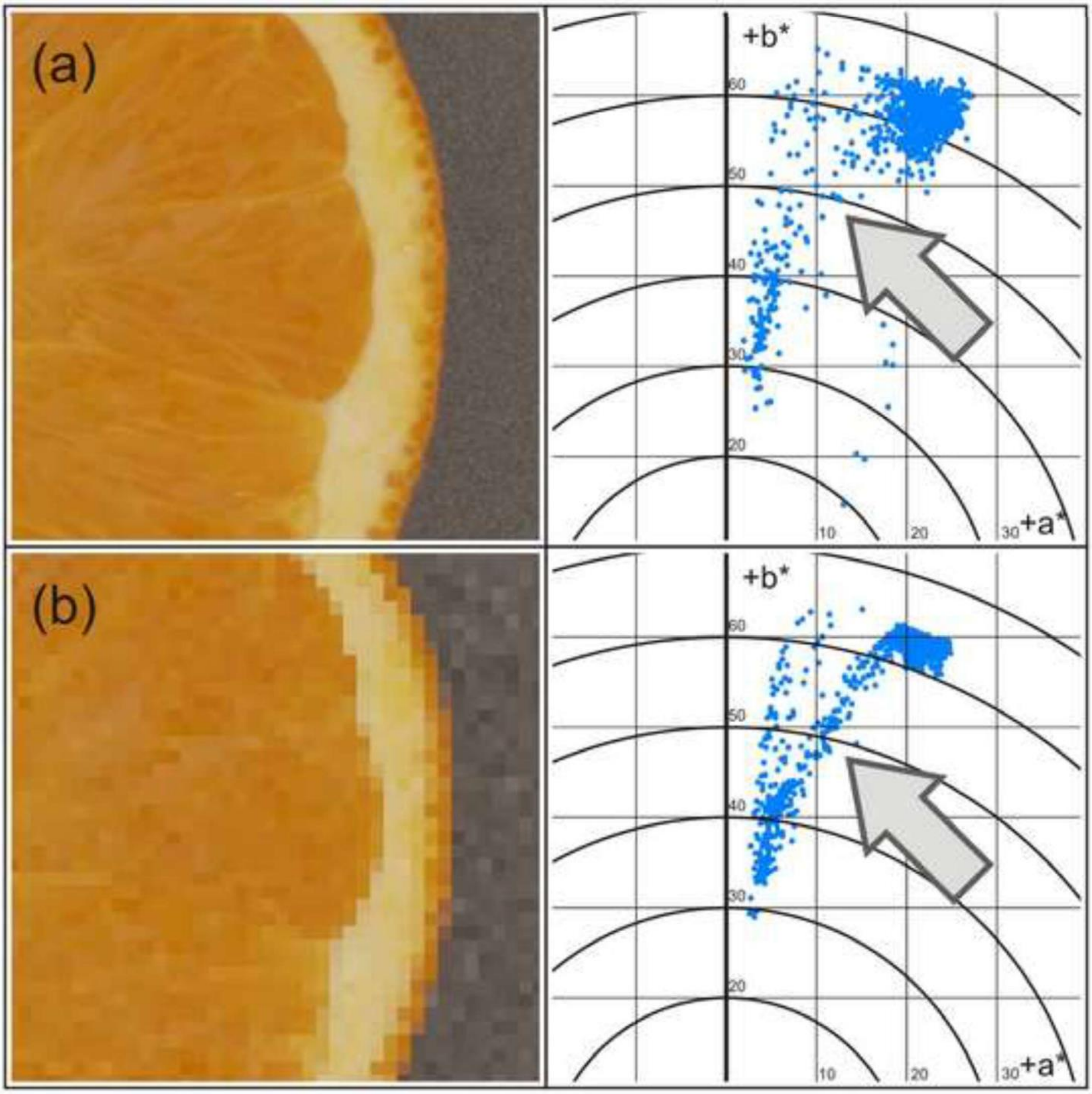

Figure 3

Click here to download high resolution image

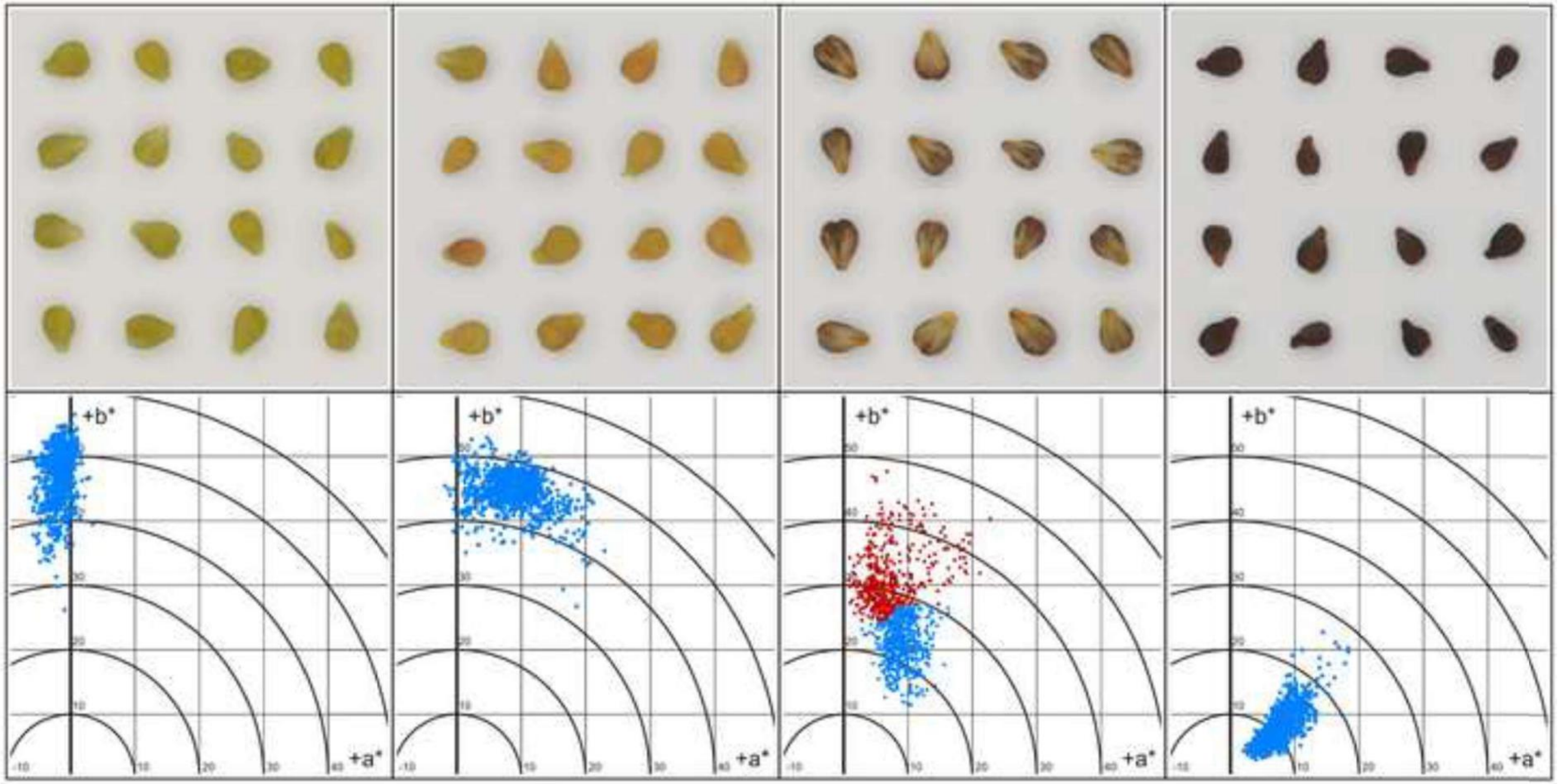

(a) (b) (c) (d)

Figure 4
Click here to download high resolution image

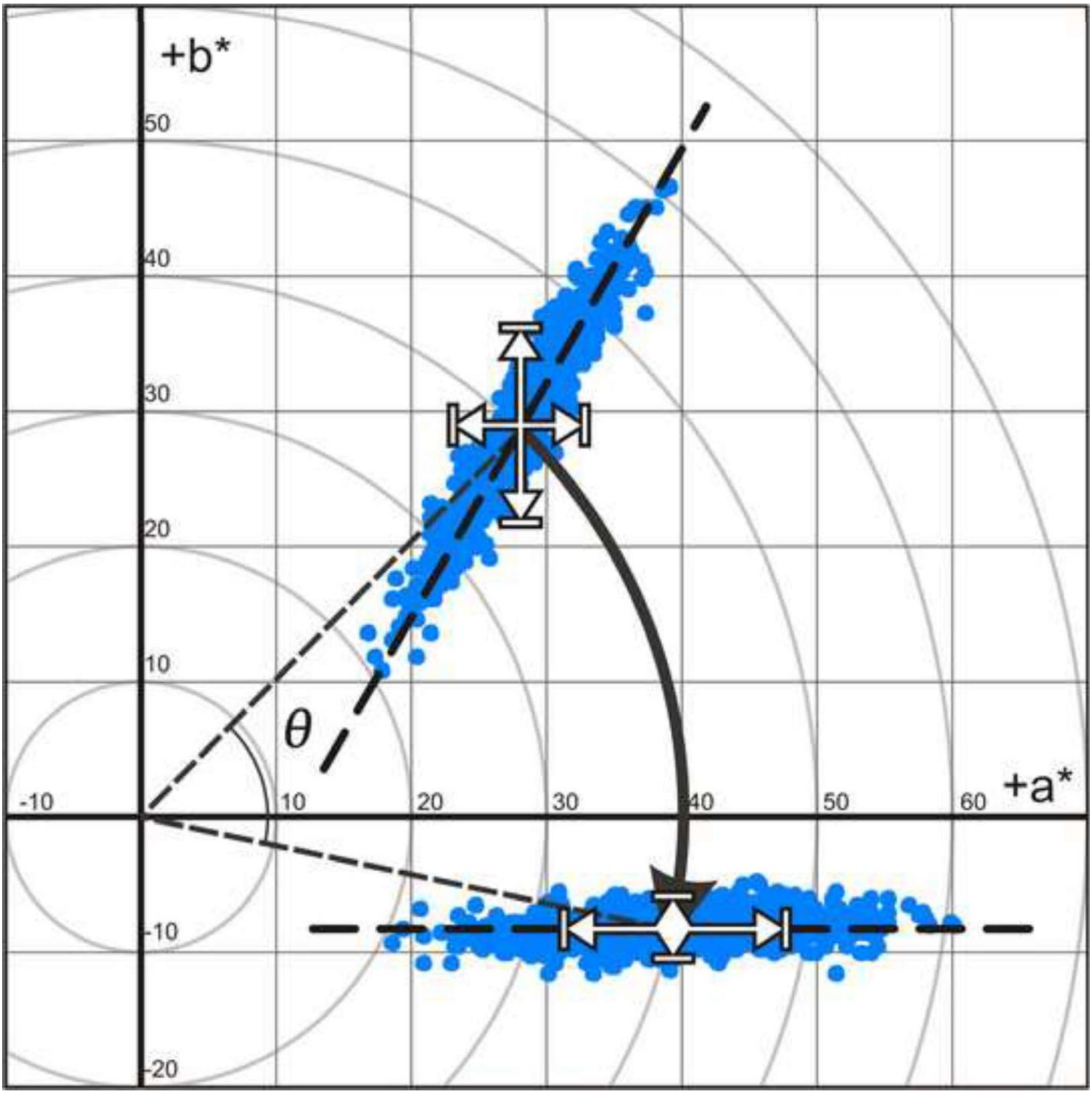

Figure 5
Click here to download high resolution image

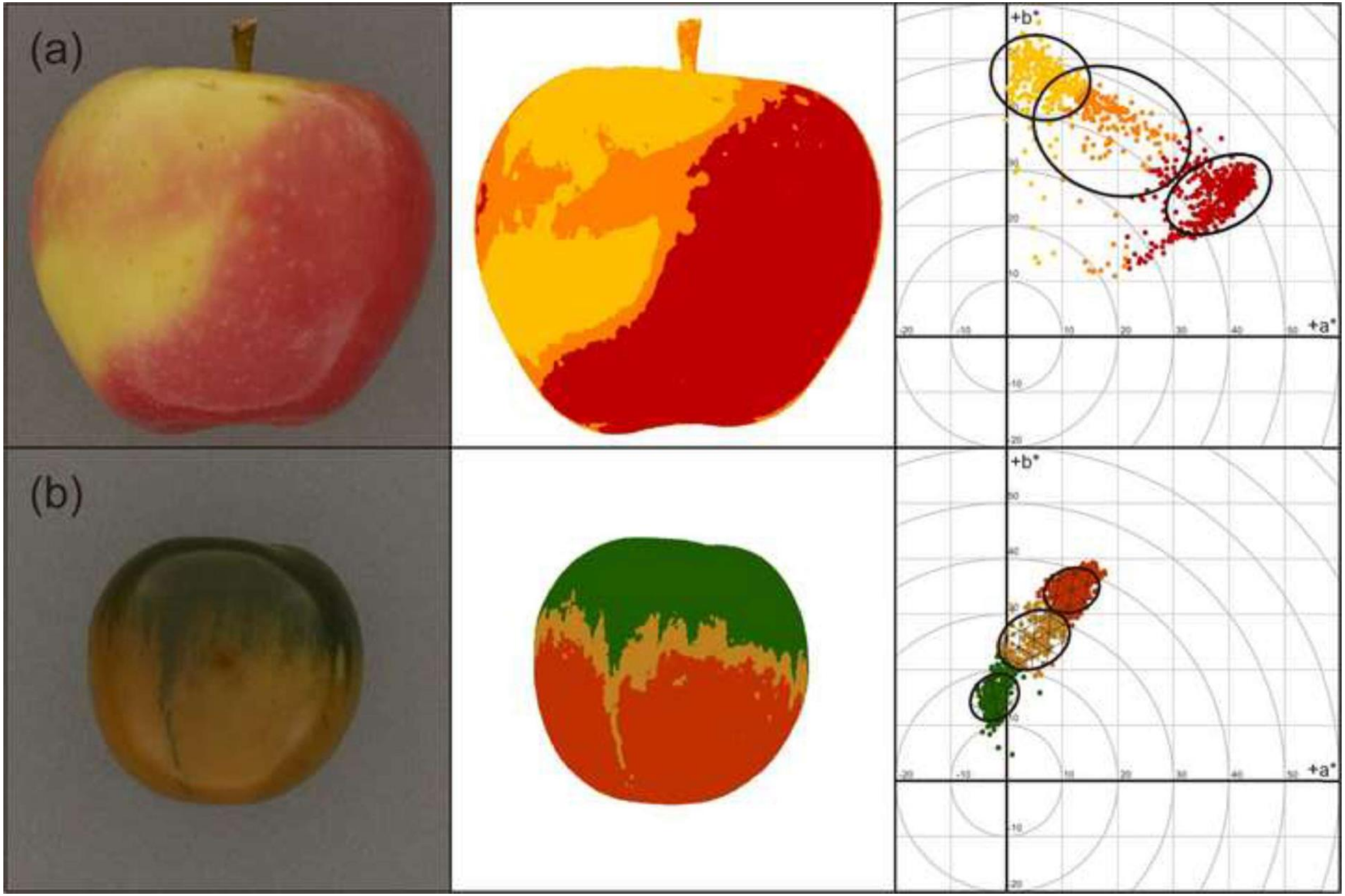

Figure 6
Click here to download high resolution image

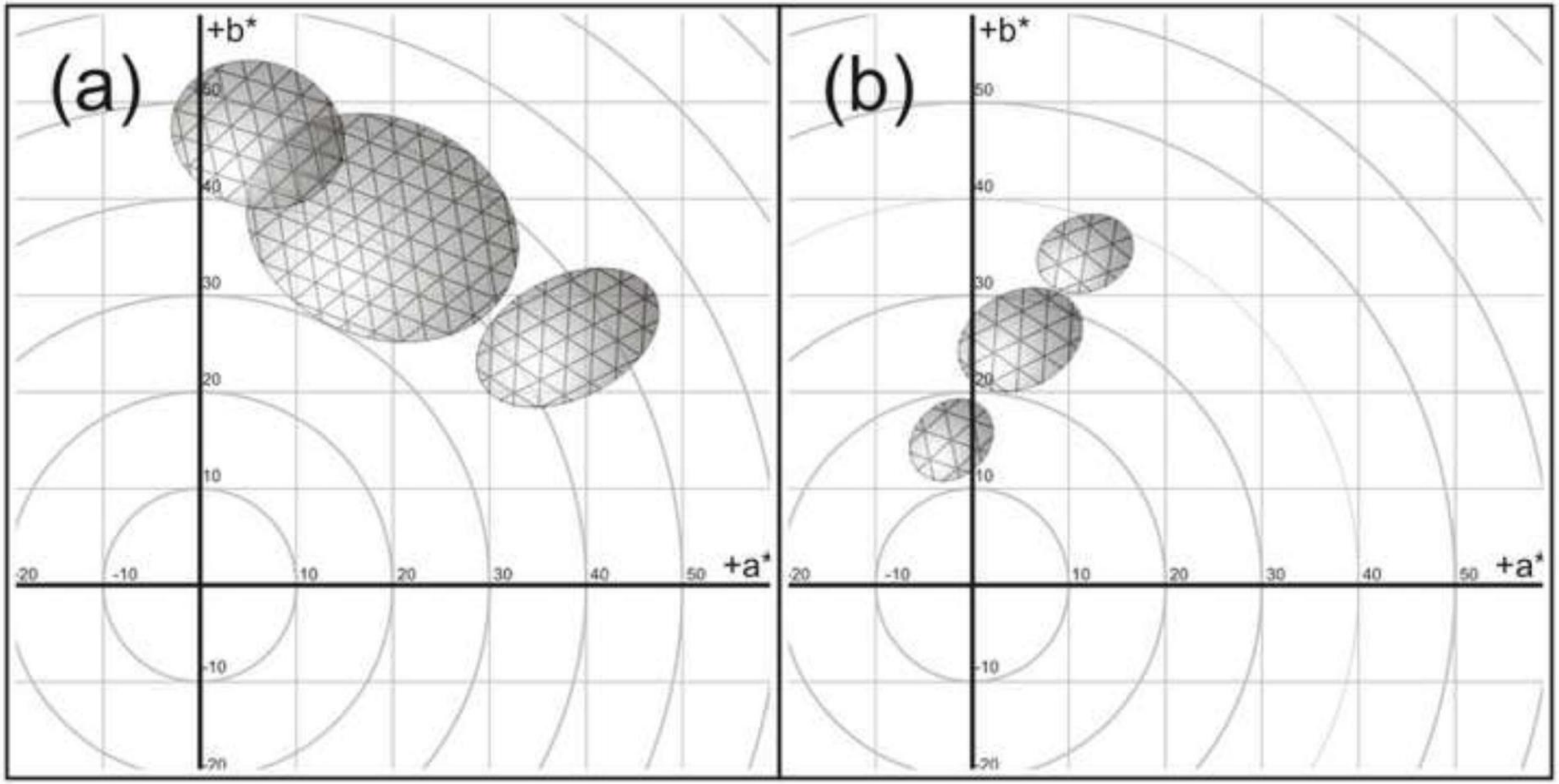

Figure 7
Click here to download high resolution image